In Situ Observation of Epitaxial Polymorphic Nucleation of the Model Steroid Methyl Analogue 17 Norethindrone

S. X. M. Boerrigter, C. J. M. van den Hoogenhof, H. Meekes,* P. Bennema, and E. Vlieg

RIM Laboratory of Solid State Chemistry, Faculty of Science, University of Nijmegen, Toernooiveld 1, 6525 ED Nijmegen, The Netherlands

P. J. C. M. van Hoof

N.V. Organon, P.O. Box 20, 5340 BH Oss, The Netherlands

Received: September 10, 2001; In Final Form: March 1, 2002

Using in situ polarization microscopy and in situ Raman spectroscopy, a polymorphic phase transition from the triclinic to the monoclinic crystal form of 7-α-methyl-Δ5,10-norethindrone has been observed in acetone solutions at room temperature. The metastable triclinic form is nucleated epitaxially on the stable monoclinic form beyond a threshold supersaturation. The metastable phase transforms into the stable phase by a solid−solute−solid mechanism in acetone. The thermodynamics of ordinary and epitaxial nucleation are discussed.

1. Introduction

A compound capable of crystallizing into different crystalline forms, or crystal structures, is said to exhibit polymorphism. Physical properties of different polymorphs can vary significantly. Solubility, melting point, density, hardness, crystal shape, optical and electrical properties, vapor pressure, etc. can be affected. The concept of polymorphism has changed significantly since the time when Ostwald formulated his rule of stages[1] which describes the appearance of metastable polymorphs in crystallization processes. Nowadays, it is understood that in many ways different polymorphic forms can coexist (i.e., exist concomitantly) as was reviewed by Bernstein et al.[2] Although not always observed, in principle, every molecular compound could turn out to be polymorphic as was already claimed by McCrone[3] (see also ref 4). Obviously, the relative stability and the involved kinetics in the formation of alternative crystal structures determine whether these show up or not. A clear example of this is the fact that the polymorph grown often depends on the solvent used. Kinetics in crystal growth processes introduce the need to look beyond equilibrium thermodynamics.

If one can obtain polymorphs of a molecular compound, one can thus manipulate the physical properties of the solid state without changing the chemical composition. This shows why the understanding and control of polymorphism is lucrative. Because a large percentage of drugs exhibits polymorphism,[5] this topic is especially interesting for the pharmaceutical industry.

Here we study the polymorphic system of the steroid 7αMNa (or in full (7α,17α)-17-hydroxy-7-methyl-19-nor-17-pregn-5(10)-en-20-yn-3-one; see Figure 1) which is used as the active ingredient in medicines for hormone replacement therapy. Two polymorphs of 7αMNa are known, a monoclinic and a triclinic form. The crystal structures of the polymorphs have been elucidated by Declercq et al.[6] and by Schouten and Kanters,[7] respectively (see Table 1 for some details).

We find that 7αMNa is an enantiotropic system and that a polymorphic phase transition can occur in the presence of acetone. We also find that beyond a modest supersaturation the triclinic form nucleates on the monoclinic form, a phenomenon we call polymorphic epitaxial growth. This phenomenon was reported by Boistelle and Rinaudo[8] for a pseudopolymorphic system. They showed that the anhydrous and the hydrated uric acid phases can nucleate and grow on top of each other. Their results prove to be quite similar to our polymorphic compound.

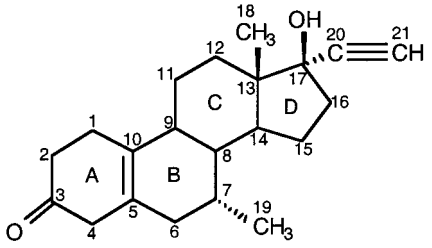

Figure 1. 7αMNa molecular structure showing standard carbon numbering and ring identification.

TABLE 1: Crystallographic Parameters of the Two Polymorphic Crystal Forms of 7αMNa

polymorph	monoclinic	triclinic
CSD refcode[20]	CIYRIL00	CIYRIL01
space group	$P2_1$	$P1$
cell dimensions	$a = 6.53$ Å	$a = 6.54$ Å
	$b = 41.21$ Å	$b = 6.68$ Å
	$c = 6.67$ Å	$c = 10.29$ Å
	$\alpha = 90°$	$\alpha = 87.1°$
	$\beta = 101.5°$	$\beta = 80.1°$
	$\gamma = 90°$	$\gamma = 79.2°$
Z′	2	1
Z	4	1

2. Thermodynamics of Polymorphism

2.1. Monotropic versus Enantiotropic Systems and Their Kinetics. A system of two polymorphs can be either monotropic or enantiotropic. In a monotropic system, the higher melting polymorph is the most stable form over the entire temperature range. Spontaneous polymorphic transformations can only occur from the metastable to the stable form. In an enantiotropic

* To whom correspondence should be addressed. E-mail: hugom@sci.kun.nl.

10.1021/jp0134547 CCC: $22.00
Published on Web 04/17/2002

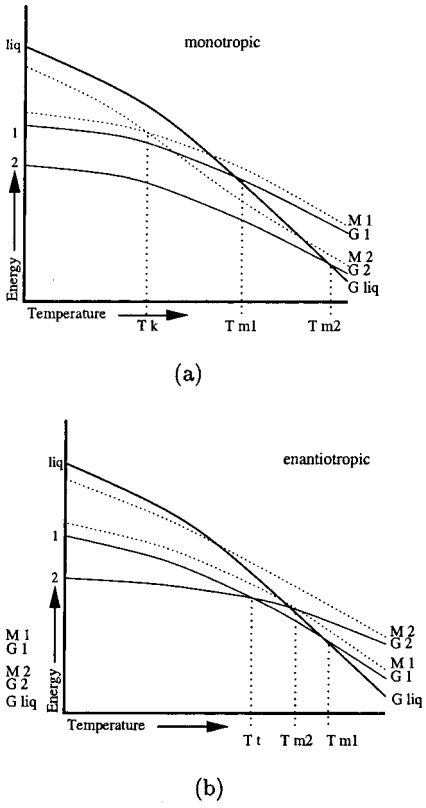

Figure 2. Hypothetical energy versus temperature curves for a monotropic polymorphic system (a) and an enantiotropic polymorphic system (b) after Burger and Ramberger. Both graphs show the Gibbs free energy (G) curves for polymorphs 1 and 2 and the liquid phase (liq) as well as the effective energy barrier causing the metastable zones M_1 and M_2 which are given by the sum of G and the activation barrier $G^{\ddagger}$. The melting points (T_m) of polymorphs 1 and 2 are indicated. The transition point (T_t), at which both polymorphs have the same Gibbs free energy only occurs in the enantiotropic system. The hypothetical metastable zones are not necessarily parallel to the Gibbs free energy curves. This gives rise to a kinetic transition temperature T_k in a at which the nucleation barrier of the two phases cross. In b, no T_k occurs which shows that even an enantiotropic system does not necessarily show polymorphism.

system, a transition temperature is found at which the Gibbs free energy curves cross.

Burger and Ramberger[9] provided considerable insight into polymorphic systems by noting, among others, the heat of transition rule (HTR). The heat of transition rule states that the two forms are related enantiotropically if an endothermal transition is observed before the sample melts while heating it. Free energy diagrams are helpful to understand such rules (see Figure 2). The HTR only holds when the enthalpy curves (not denoted here) of both polymorphs do not cross. Burger and Ramberger examined 113 polymorphs.[10] In more than 99% of the cases, the HTR turned out to hold.

In addition to their thermodynamical considerations, in Figure 2, hypothetical metastable zones are drawn indicating the kinetic barriers encountered during crystallization. The metastable zones of the two phases depend mainly on the temperature and the solvent. The zones most likely broaden at lower temperatures, but the broadening depends on the crystallization process and therefore on the particular polymorph, which may cause the metastable zones of different polymorphs to cross. Furthermore, the widths and relative positions of the metastable zones can change completely for different solvents. This causes different polymorphs to be selectively grown from different solvents, which is frequently observed. It is obvious that the various possible arrangements of the Gibbs free energy curves of polymorphic phases and their metastable zones can give a wide variety of polymorphic behavior and causes polymorphs to exist concomitantly in various stages of crystal growth. For an excellent overview of examples by Bernstein et al., see ref 2. A discussion on the role of the solvent for the metastable zones was recently given by Threlfall.[11]

2.2. Types of Kinetics. Because metastable zones are caused by kinetics, it is very important to notice that several types of kinetics play a role in crystal nucleation which can be divided into two groups. The first involves mobility kinetics, and the second involves the barrier of forming nuclei. Mobility kinetics involve the movement of molecules of the crystallizing material as well as of the solvent during crystallization. As an example, the solvent layer may impose an orientational effect on the solute molecules with respect to the crystal surfaces as is shown for instance for urea by Boek et al.[12−14] Another very important type of mobility kinetics involves the molecular conformations. It is believed that the growth kinetics are enhanced if the preferred conformation in solution resembles the conformation in the crystal. All kinds of mechanism involved in mobility kinetics determine the rate of the processes taking place.

The barrier of formation of nuclei can be divided into the 3D and 2D nucleation barriers. The 3D barrier is governed by the balance between bulk and surface energies of the nuclei, and for 2D, the barrier is governed by the balance between the bulk and edge energies of the 2D nuclei. At its maximum, the energy versus nucleus size curve yields the critical nucleus. In general, the larger the critical nucleus, the larger its metastable zone. In practice, the two types of kinetics cannot be separated. A smaller critical nucleus does not necessarily mean that it will be created more quickly because of the mobility kinetics. Moreover, the surface energy of either type of nuclei is moderated by solvents as they interact with the surface.

We should note that the presence of impurities can dramatically change the metastable zone width as well. These impurities can be chemical compounds in the solution or physical impurities such as dust particles. Even the walls of the crystallization container must be regarded as a nucleation inducing factor narrowing the metastable zone width. It is well-known that working at purer conditions broadens the metastable zone considerably, and it is extremely difficult to rule out this effect completely.

2.3. 3D Nucleation Kinetics. The necessity to create a critical 3D nucleus results in different metastable zones for different polymorphs. The metastable zones determine which polymorph crystallizes and indicates the threshold supersaturation which has to be applied to obtain homogeneous nucleation [Nyvlt, J. *Cryst. Res. Technol.* **1995**, *30* (4), 443]. The consequences for the nucleation of polymorphs for various arrangements of the metastable zones have been discussed by Threlfall for different temperatures and in the presence or absence of a seed crystal.[11]

For small systems such as our growth vessels, a well controlled slow increase of the supersaturation can experimentally be maintained. Starting from the undersaturated situation for both polymorphs, by evaporation, lowering the temperature, or adding an antisolvent, the effective concentration of the solute can be increased in a precisely controlled way.

2.4. 2D Nucleation Kinetics. 2D nucleation kinetics mainly determine the growth mechanism and growth speed of a surface. At moderate supersaturation, this involves the homogeneous process of a birth and spread mechanism involving the creation of 2D nuclei on the surface. The dislocation (spiral) mechanism circumvents this which effectively lowers the 2D nucleation

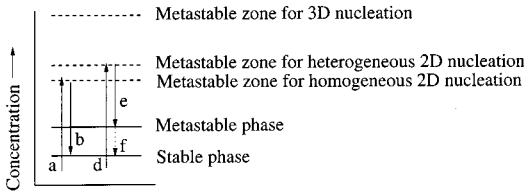

Figure 3. Schematic representation of the various nucleation barriers as a function of the concentration. The arrangement of the nucleation concentrations is chosen to represent a system capable of polymorphic heterogeneous 2D nucleation. a-f denote the possible trajectories of crystallization as a result from an increase in concentration.

barrier, allowing growth at lower supersaturations. In this work, a particular type of 2D heterogeneous nucleation plays a key role. The only difference from homogeneous nucleation is that a different polymorph nucleates. We will call this the heterogeneous 2D nucleation of the metastable polymorph.

This process will easily take place if the energy barrier of heterogeneous 2D nucleation is low. However, it must be higher than the energy barrier of the ordinary 2D homogeneous nucleation of the stable phase, otherwise the stable phase would not crystallize in the first place. Therefore, this heterogeneous growth is only expected to be seen at sufficiently high supersaturations, i.e., higher than the heterogeneous nucleation concentration. Figure 3 demonstrates this by two alternative trajectories. In this figure, the concentration is assumed to be too low (small supersaturation) for 3D nucleation to be effective. A seed crystal of the stable polymorph, however, is present. The a−b trajectory shows the regular homogeneous 2D nucleation and growth of the stable phase on the seed crystal. The d−e trajectory shows the epitaxial polymorphic nucleation process. It shows that from this scheme the metastable phase is only expected to be seen if step e is significantly faster than step b, and, additionally, the transformation (step f) is sufficiently slow. The rate of the steps in the trajectory are governed by the mobility kinetics. Effectively, this means that, in order for the newly created metastable phase not to be overgrown by the stable, the mobility kinetics of the metastable phase must be more favorable than that of the stable phase.

Metastable crystalline material will tend to transform into the stable form (step f) which implies a solid−solid-phase transition. Nývlt, however, described the kinetics of a solid−liquid−solid-phase transition in detail.[15] He showed that this mechanism has much faster mobility kinetics. In our case, the mechanism of the transition is mediated by a solvent layer which proceeds through the crystal. At one side, the metastable phase dissolves, and at the other side, the crystal immediately recrystallizes as the stable phase. Therefore, the transition could rather be regarded as a solid−solute−solid transition. Liquid mediated phase transition are known. A nice example is the transition from phase III to IV in NH_4NO_3, which has been studied in detail.[16,17] Nývlt also mentions the importance of the induction period which is caused by the necessity to create the solute layer, i.e., initiate the recrystallization front.

Obviously, it is important to know the "width" of the various metastable zones to be able to understand the crystallization phenomena of a compound in detail. It is clear that by conducting crystallization experiments and monitoring the phases of the growing crystals it is possible to establish some insight into the various metastable zone widths.

2.5. Solubility. As a good energy reference for polymorphs, the melts, vapors, and solutions prepared from these polymorphs can be considered. These phases are independent from the polymorphs as they are formed by the individual molecules not showing any crystallinity. Solubility measurements are, therefore, very useful. The difference in dissolution Gibbs free energy of two polymorphs equals the difference in the fusion Gibbs free energies of both polymorphs. It can easily be seen from free energy diagrams that the thermodynamically less stable polymorph has a smaller energy of dissolution than the more stable polymorph. The polymorph with the smaller dissolution Gibbs free energy has a higher solubility and vice versa. The relation between the dissolution Gibbs free energy (ΔG^{diss}) and the solubility x given as the molar fraction is

$$\ln x = -\frac{\Delta G^{\mathrm{diss}}}{RT} = -\frac{\Delta H^{\mathrm{diss}}}{RT} + \frac{\Delta S^{\mathrm{diss}}}{R} \qquad (1)$$

By plotting the solubility data in a classical Van't Hoff plot (the logarithm of the solubility versus the reciprocal of the absolute temperature), we can obtain the dissolution enthalpy ΔH^{diss} and entropy ΔS^{diss} from the slope of the solubility curve and the intercept with the y axis, respectively. It is important to note that eq 1 is based on the assumption that the solution is regular; that is, the solution has a nonzero enthalpy of mixing and an ideal mixing entropy.[18]

In the next sections, in situ crystallization experiments of 7αMNa in acetone will be presented and discussed. It will be shown that the metastable zones play an important role during both homogeneous nucleation and heterogeneous nucleation, either 3D or 2D.

3. Experimental Section

3.1. Materials. The steroid 7αMNa was kindly supplied by N. V. Organon. The starting material has a monoclinic structure. To obtain triclinic crystals, the material was recrystallized in *n*-hexane. All solvents used were analytical reagent grade or better.

3.2. Crystal Growth. The crystal growth experiments were conducted in an in situ cell.[19] This closed glass cell contains a fixed amount of compound and solvent to ensure that the saturation temperature of the system is exactly known and remains constant. An optical transmission microscope equipped with polarization filters was used to observe the crystals in the glass cell. To prevent degradation of the 7αMNa, only green light was used. Using a thermostated water bath, the temperature of this cell and its contents could be lowered and raised below and above the saturation temperature of the 7αMNa solution. After all of the solid material of the starting solution was dissolved, high supersaturations were imposed ($\Delta T = 20$ °C; $\sigma \approx 0.5$) to nucleate crystals. Subsequently, all crystals except one were dissolved by heating the cell to a mild under-saturation. The remaining crystal was dissolved until its volume was very small compared to the volume of the cell. The change of concentration in the solution was therefore negligible at this stage, and the saturation point, or equilibrium temperature, could be determined. At the saturation point, the temperature is such that neither growth nor dissolution occurs. Its value could be refined using the optical microscope over a longer period of time. The relative error was within 0.1 K.

3.3. Raman Spectroscopy. The in situ cell was also used for microscopic Raman measurements to determine the polymorphic modification of a crystal. The Raman setup used consisted of a Dilor XY multichannel spectrometer with a 514.5 nm Ar^+ ion laser excitation source. The 1800−1600 cm^{-1} region was found to be most suitable to distinguish in situ between the monoclinic and the triclinic modification of 7αMNa crystals in the acetone solution. The triclinic polymorph shows a single

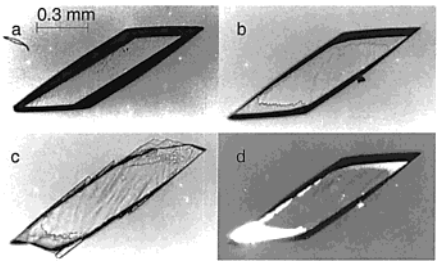

Figure 4. Optical micrographs of an 7αMNa crystal grown from acetone solution at low, $\sigma \approx 0.06$ (a), and high supersaturation, $\sigma \approx \sigma^* \approx 0.13$ (b) and (c). In d, a polarization microscope photograph of the crystal in b is shown; the layer on top of the crystal illuminates, whereas the underlying crystal is oriented in its extinction position.

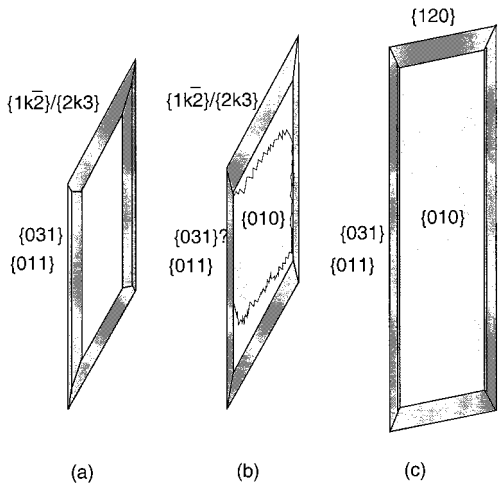

Figure 5. Schematic drawing of the morphology of 7αMNa crystals grown at low supersaturation, $\sigma \approx 0.06$ (a), intermediate supersaturation, $\sigma \approx \sigma^* \approx 0.13$ (b), and at high supersaturation, $\sigma \approx 0.26$, after waiting for several days (c).

peak at 1662 cm^{-1}, whereas the monoclinic polymorph exhibits two peaks at respectively 1660 and 1665 cm^{-1}. These peaks are attributed to the double bond stretch vibration between carbons 5 and 10 (see Figure 1). The peak doubling of the monoclinic form is caused by conformational differences. The asymmetric unit of the monoclinic form consists of two conformers of the steroid mainly differing in the adjacent carbonyl holding ring (A) which can exist in two-half-chair conformations. The monoclinic form has both, whereas the triclinic form only has one conformation. The carbonyl peaks at 1710 (monoclinic) and 1720 cm^{-1}(triclinic) are covered by that of the acetone which makes them useless for in situ purposes.

4. Results and Discussion

4.1. Crystal Growth and Morphology. Figure 4 shows four photographs of the same 7αMNa crystal during growth in an acetone solution. The crystal in Figure 4a was grown by leaving a nucleus, obtained by the method described in section 3.2, during 24 h at low supersaturation ($\sigma \approx 0.06$).

When the supersaturation was increased above a certain threshold value ($\sigma > \sigma^*$; $\sigma^* \approx 0.13$), a new layer started to grow on the crystal (Figure 4b). In all observed cases, the layer started at the short sides of the needle shaped crystal. After the top face was completely covered, this layer grew over its borders in a fairly rough fashion (see Figure 4c). When parts b and c of Figure 4 are compared, it can be seen that the overall angle between the short and long sides of the crystal has become much

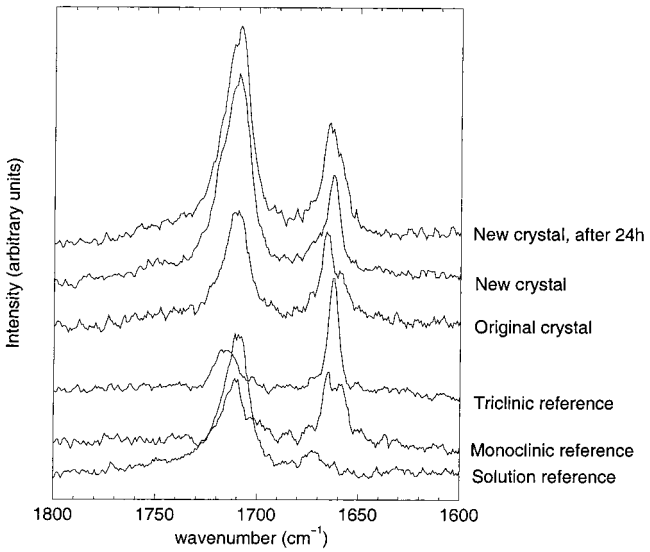

Figure 6. Raman spectra of the original crystal, the new crystal just after nucleation, and after 24 h as presented in Figure 4.

less sharp. When this crystal was left for several days at high supersaturation, a large crystal of about 10 × 2 × 2 mm was obtained (Figure 5c).

Ex situ determination of the morphology of the original crystal in Figure 4 parts a and b was not possible because of the microscopic setup and an extreme shutoff effect. The indexation given in Figure 5 parts a and b is therefore based on the in situ measurements of the angles between the faces. Therefore, the form at the short side of the crystal could not be indexed definitely. However, the large crystal obtained by growing for several days at high supersaturations, could be indexed using a goniometer (Figure 5c).

The large crystal dissolved after lowering the supersaturation below σ^*. The saturation temperature of this crystal is therefore different from that of the original crystal. Using polarization microscopy, we found that the newly formed layer on top of the {010} face of the original crystal had a different extinction orientation (see Figure 4d). Combined with the observation of different saturation temperatures of the two crystals, this implies that the crystalline material at this spot is another phase. This suggests the phenomenon of polymorphic epitaxial growth.

4.2. In Situ Raman Measurements. To test the phenomenon of polymorphic epitaxial growth, in situ Raman measurements were performed. The peak doubling at 1662 cm^{-1} which is typical for the monoclinic phase cannot be seen in the spectrum of the new crystal whereas it is present for the original crystal (Figure 6). During a period of 24 h, the spectrum of the new crystal gradually changed toward the monoclinic spectrum. Although the shoulder at lower wavenumber is not clearly visible yet, the bigger peak has shifted back to its original position. From these results, it can be concluded that the original crystal is monoclinic. During its growth, the new crystal showed a dominating triclinic structure, which slowly transformed into the monoclinic structure. This agrees with the hypothesis in section 4.1. Because the in situ spectra all contain the solution peak, ex situ single-crystal X-ray measurements were conducted as a final check. This showed that the final structure of the new crystal was indeed monoclinic.

Note, that it is impossible to determine the phase of the first homogeneously nucleated crystals as they are too small for that and they will transform readily into the monoclinic form.

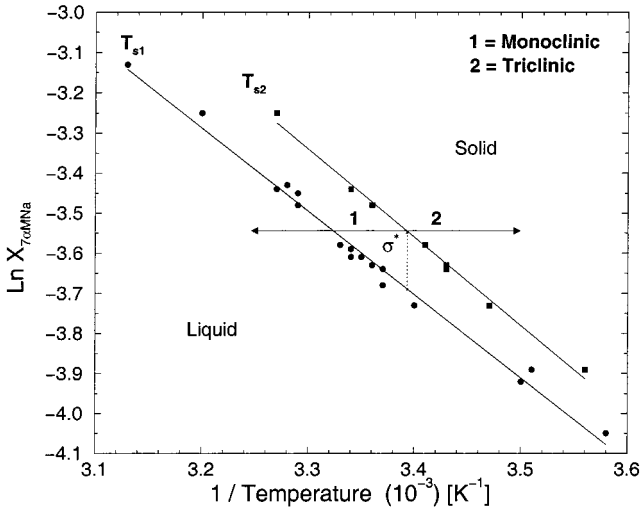

Figure 7. Solubility curves of 7αMNa in acetone solution for the monoclinic polymorph (T_{s1}) and the triclinic polymorph (T_{s2}). In the area marked 1 ($\sigma < \sigma^*$), between both saturation lines, the monoclinic polymorph nucleates homogeneously, and in the area marked 2 ($\sigma > \sigma^*$), the triclinic polymorph nucleates epitaxially.

4.3. Solubility Measurements. For both polymorphs, the saturation temperatures of 7αMNa solutions with varying concentrations were measured. The results are shown in Figure 7.

By using eq 1, the heats of dissolution and the dissolution entropies of both polymorphs were determined assuming a regular solution:

$$\text{monoclinic: } \Delta H^{\text{diss}} = 17.3 \pm 0.5 \text{ kJ/mol}, \quad \Delta S^{\text{diss}} = 28.00 \pm 0.05 \text{ J/mol K}$$

$$\text{triclinic: } \Delta H^{\text{diss}} = 18.3 \pm 0.6 \text{ kJ/mol}, \quad \Delta S^{\text{diss}} = 32.66 \pm 0.07 \text{ J/mol K}$$

Figure 7 shows that both solubility curves intersect somewhere at the far right of the graph, which yields a transition temperature of -52 ± 36 °C. This implies that 7αMNa is enantiotropic. However, the error in the transition temperature is quite large. Therefore, DSC measurements were performed on 7αMNa to obtain conclusive results. The thermogram of the monoclinic polymorph, measured at 5 °C/min, exhibits only one endothermal peak at $T = 170$ °C: its melting peak. The thermogram of the triclinic polymorph shows an additional endothermal peak at $T = 144$ °C. IR hot stage microscopy showed that this peak corresponds to the transition from the triclinic to the monoclinic phase. According to the HTR, an endothermal peak means that the system is indeed enantiotropic. The HTR also states that the thermodynamical equilibrium temperature must be lower than the experimental temperature of an endothermal transition. This hysteresis effect appears to be extremely large in our case, because DSC runs showed that the phase transition is not reversible down to room temperature, which was already expected from the solubility measurements. Therefore, the exact transition temperature could still not be determined. The possibility of hysteresis is supported by the fact that larger heating rates show higher transition temperatures. Although not determined accurately, it suffices to know that the transition temperature is well below 0 °C; the two solubility curves in Figure 7 can be considered to run parallel within a very good approximation, making the value of σ^* constant in a temperature region of practical relevance.

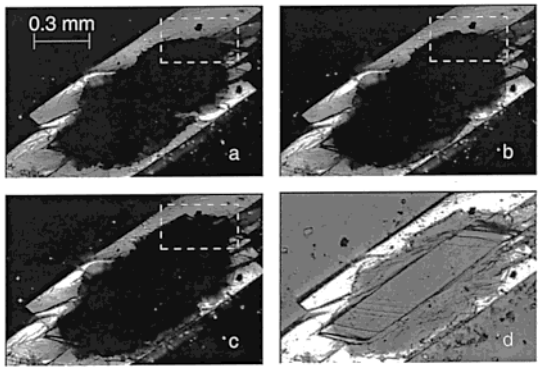

Figure 8. Polarization micrographs of the transition of the triclinic into the monoclinic modification at $t = 0$ (a), 10 (b), and 20 min (c). In d, one of the polarization filters was turned a few degrees out of its extinction orientation, clearly showing the original crystal.

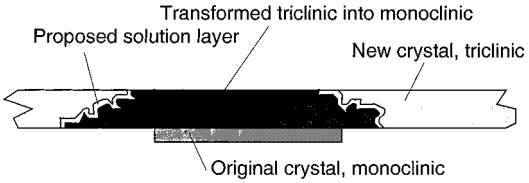

Figure 9. Schematic representation of the hypothetical position of the original crystal and the epitaxially nucleated crystal on top of it. The proposed solution layer proceeds through the crystal transforming the triclinic into the monoclinic phase.

4.4. Polymorphic Phase Transition. The transformation of the triclinic phase into the monoclinic one could be followed in situ by polarization microscopy. A monoclinic crystal similar to that of section 4.1 was taken on which the triclinic phase was nucleated. The monoclinic phase was oriented to show extinction. Figure 8a−c shows that the extincted (black) area slowly expanded with time; especially at the indicated boxed area. This shows that the transformation of the triclinic (not extincted) into the monoclinic modification slowly progressed through the crystal. The edges of this transformation front did not appear to be faceted.

Both polymorphs are stable if stored cool and dry and have shelf lives of years. Moreover, the DSC results show that a temperature of 144 °C is needed to induce the phase transition, which must follow a solid−solid mechanism because the samples used for DSC were dry. Our experiments show that the phase transition takes place at much lower temperatures in the solution as well as in the presence of acetone as will be described in section 4.5. It is therefore concluded that the phase transition follows a solid−solute−solid mechanism which proceeds through the crystal (see also Figure 9). A solid−solid transition can, however, not be ruled out completely because the proposed solvent layer (i.e., the presence of acetone in the recrystallization front) could not be observed through the microscope.

Because both the transformed crystal areas and the original crystal extinct in the same orientation by polarization microscopy, the crystal orientations of both must be identical. The dark area in Figure 8 is larger than the original crystal as can be seen in Figure 8d, where it is clearly visible and exhibits well defined edges and facets. An interesting observation is that the original crystal kept growing in this condition. It was found that the original crystal was positioned underneath the new crystal rather than being completely surrounded by it as is schematically represented in Figure 9. This also shows that the epitaxial growth selectively takes place on the {010} form. This can be understood by comparing the *ac* plane of the $P2_1$ and

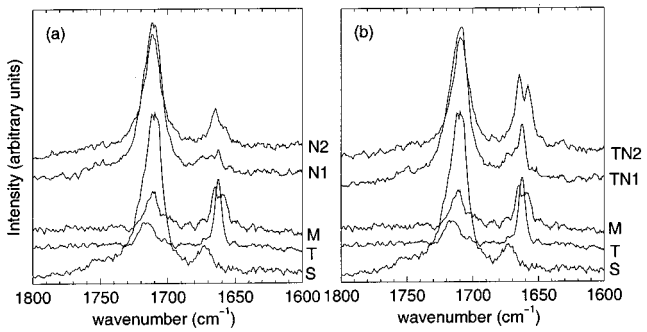

Figure 10. Raman measurements of primary nucleation in area 2 (a) and measurements of a triclinic needle placed in the in situ cell at high supersaturations ($\sigma > \sigma^*$) (b). M = monoclinic reference, T = triclinic reference, S = solution reference, N1 = nucleus at $\sigma > \sigma^*$, N2 = nucleus at $\sigma > \sigma^*$ after 24 h, TN1 = triclinic needle just after addition, and TN2 = triclinic needle after 48 h.

the *ab* plane of the *P*1 polymorphs which turn out to be nearly identical (lengths vary only by 0.01 Å, the angle by $|90 - \beta_{P2_1}| - |90 - \gamma_{P1}| = 0.7°$; see Table 1). The molecular orientations in the crystal structure of the two phases are nearly identical at the interface layer thus maintaining the hydrogen bridge bonding scheme. This causes the interfacial layer between the two phases to be relatively stable, which according to the theory is a requirement for the heterogeneous epitaxial nucleation.

To examine the role of the monoclinic phase on the solid−solute−solid transformation mechanism, Raman measurements were conducted on the epitaxially grown crystal as well as on a triclinic needle grown from an hexane 7αMNa solution. For this, they were placed in the in situ cell at high supersaturation ($\sigma > \sigma^*$) and left for several days. The results are presented in Figure 10 parts a and b. Although the measured intensities of the epitaxially nucleated crystal is low because of its small thickness, it does confirm that the triclinic primary nucleus transformed into the monoclinic polymorph as the peaks of both phases are just visible. The triclinic needle clearly transformed into the monoclinic phase. This proves that the presence of the monoclinic phase is not necessary for the transformation and, thus, that the solid-solute-solid mechanism initiates within 24 h.

4.5. Solid−Solute−Solid-Phase Transition. Apparently, the presence of acetone speeds up the transformation enormously. As was shown in previous sections, this is caused by a solid−solute−solid mechanism. To test the role of the solvent in the phase transition, several experiments were carried out using various combinations of crystals and solvents. The phase transitions were observed ex situ using X-ray powder diffraction before and after at least 24 h after adding the solvent.

As a first test, a few droplets of pure acetone were added to a pure triclinic 7αMNa sample and subsequently left in a closed vessel for 24 h. This was also done with a few droplets of a saturated 7αMNa acetone solution. In both cases, the samples transformed into the monoclinic phase (see Figure 11 parts a and b, respectively). The saturated solution shows that the process does not depend on the solvation of a substantial amount of crystal at the addition stage.

Similar experiments using open vessels hardly showed any transformation even after two additions of solvent and a total time of 48 h. This is caused by the evaporation of the acetone droplets typically within a minute. In contrast, a 50:50% mixture of triclinic and monoclinic 7αMNa showed that the mixture changed to approximately 30:70% after the first addition and to 0:100% after the second addition. This shows that the transformation rate is dramatically enhanced by the presence

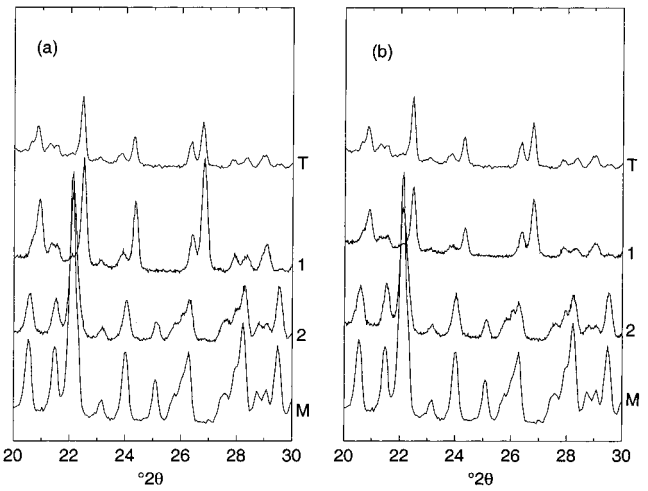

Figure 11. A few droplets of acetone (a) and saturated 7αMNa solution (b) were added to a pure triclinic sample. X-ray powder diffraction measurements were conducted before addition (1) and after leaving it for 24 h in closed vessels (2). M = monoclinic reference, and T = triclinic reference

of the monoclinic phase. We believe that this enhancement can be understood by the fact that the initiation of the monoclinic boundary layer is not necessary in the mixture and that the initiation of the monoclinic boundary layer hardly takes place on the pure triclinic samples.

All these experiments are consistent with the hypothesis of the solid−solute−solid mechanism which is therefore considered to be very relevant for the phase transition behavior of the polymorphic epitaxial layer. Once the process is initiated, a recrystallization front moves through the crystal via a liquid boundary layer. The initiation of a boundary layer proves to be a limiting step in the process.

5. Conclusions

The enthalpies of dissolution of the two polymorphic forms of 7αMNa are different only by about 1 kJ/mol. Because of this, experimental conditions can be found where both polymorphs can be grown from the same solvent at the same temperature. The difference in supersaturation has been shown to be decisive upon the polymorph formed. Equilibrium thermodynamics cannot explain these results. Hence, kinetics must be the underlying cause.

It is important to know the nature of the kinetics to understand the crystal growth phenomena. First of all, we have shown that the two polymorphs form an enantiotropic system. Although the exact transition temperature could not be determined accurately, it must be well below 0 °C. It should be noted that the two structures appear to be quite similar at the interface layer of the {010} form of the monoclinic phase and the {001} form of the triclinic phase. Moreover, as a result of the small differences in enthalpies and entropies, the difference in Gibbs free energy is small in the range of the experimental temperatures (about 0.3 kJ/mol at 277 K and 0.5 kJ/mol at 322 K). Therefore, polymorphic epitaxial growth can take place in this whole range. For this phenomenon, three conditions have to be met: a low energy barrier for polymorphic nucleation, a small difference in Gibbs free energy and, as was derived in section 2.4, favorable mobility kinetics for the metastable phase. The Gibbs free energies can be close if either both enthalpy and entropy differences are small or near the transition temperature of an enantiotropic system.

Temperature and concentration are not as manageable throughout an industrial crystallization facility as it is in our laboratory scale crystal growth vessels. This causes the formation of the metastable form to be difficult to prevent in acetone. If a more suitable solvent has to be chosen rationally, one has to consider the three conditions for polymorphic epitaxial growth. When the Gibbs free energies of polymorphs of a compound are close, the options are limited to choosing solvents that favor the stable phase in terms of mobility kinetics. This is however very difficult to predict. Polymorphic epitaxial growth could be a more general phenomenon and might therefore be the cause of many polymorphic problems occurring in industrial crystallization. For this, supersaturation dependent crystallization experiments are essential to understand the nature of the phenomena.

Acknowledgment. The authors acknowledge the following persons: J. van Bentum for his help with the Raman spectroscopy, M. van der Schans for doing the DSC measurements, and C. Funke and F. Kaspersen for fruitful discussions and providing the 7αMNa. This project was supported by The Netherlands Foundation for Chemical Research (CW) with financial aid from Organon and The Netherlands Organization for Scientific Research (NWO), in the framework of the PPM/CMS crystallization project.

References and Notes

(1) Ostwald, W. *Z. Phys. Chem.* **1897**, *12*, 289.

(2) Bernstein, J.; Davey, R. J.; Henck, J.-O. *Angew. Chem., Int. Ed. Engl.* **1999**, *38*, 3440.

(3) McCrone, W. C. In *Physics and Chemistry of the Organic Solid State*; Fox, D., Labes, M. M., Weissberger, A., Eds.; John Wiley & Sons: New York, 1965; Vol. 2, pp 725−767.

(4) Dunitz, J. D.; Bernstein, J. *Acc. Chem. Res.* **1995**, *28*, 193.

(5) Kuhnert-Brandstatter, M. *Pharm. Unserer Zeit.* **1975**, *4* (5), 131.

(6) Declercq, J. P.; van Meerssche, M.; Zeelen, F. J. *J. R. Neth. Chem. Soc.* **1984**, *103* (5), 145.

(7) Schouten, A.; Kanters, J. A. *Acta Crystallogr. C.* **1991**, *47*, 1754.

(8) Boistelle, R.; Rinaudo, C. *J. Cryst. Growth* **1981**, *53*, 1.

(9) Burger, A.; Ramberger, R. *Mikrochim. Acta* **1979**, *II*, 273.

(10) Burger, A.; Ramberger, R. *Mikrochim. Acta* **1979**, *II*, 259.

(11) Threlfall, T. *Org. Proc. Res., Dev.* **2000**, *4*, 384.

(12) Boek, E. S.; Briels, W. J.; Feil, D. *J. Chem. Phys.* **1994**, *98* (6), 1674.

(13) Boek, E. S.; Briels, W. J.; van der Eerden, J.; Feil, D. *J. Chem. Phys.* **1992**, *96* (9), 7010.

(14) Liu, X. Y.; Boek, E. S.; Briels, W. J.; Bennema, P. *Nature* **1995**, *374* (23 March), 342.

(15) Nývlt, J. *Cryst. Res. Technol.* **1997**, *32* (5), 695.

(16) Davey, R. J.; Ruddick, A. J.; Guy, P. D.; Mitchell, B.; Maginn, S. J.; Polywka, L. A. *J. Phys. D: Appl. Phys.* **1991**, *24*, 176.

(17) van Driel, C. A.; van der Heijden, A. E. D. M.; de Boer, S.; van Rosmalen, G. M. *J. Cryst. Growth* **1994**, *141*, 404.

(18) Atkins, P. W. *Pysical Chemistry*, 4th ed.; Oxford University Press: New York, 1990; p 165.

(19) Vogels, L.; Marsman, H.; Verheijen, M. *J. Cryst. Growth* **1990**, *100* (3), 439.

(20) Allen, F. H.; Kennard, O. *Chem. Design Autom. News* **1993**, *8* (1), 1, 31.